ELSEVIER

Journal of Power Sources 68 (1997) 59–64

JOURNAL OF POWER SOURCES

Chemical properties of various organic electrolytes for lithium rechargeable batteries 1. Characterization of passivating layer formed on graphite in alkyl carbonate solutions

Shoichiro Mori *, Hitoshi Asahina, Hitoshi Suzuki, Ayako Yonei, Kiyomi Yokoto

Tsukuba Research Center, Mitsubishi Chemical Corporation, 8-3-1 Chuo, Ami, Inashiki, Ibaraki 300-03, Japan

Accepted 27 December 1996

Abstract

The characteristics and reaction mechanisms of the passivating film formed on the surface of graphite were investigated in ethylene carbonate–diethyl carbonate solutions containing $LiClO_4$, $LiPF_6$ and $LiN(SO_2CF_3)_2$. The electron consumption resulting on the irreversible capacity of graphite was almost equivalent to that used in the one-electron reduction of Li^+ found in the film. The electrochemical reactions in the first discharge process may be divided into the following steps: (i) 'initial film formation step' from 1.4 to 0.55 V; (ii) 'main film formation step' from 0.55 to 0.2 V, and (iii) 'lithium intercalation step from 0.2 to 0.0 V. Most of the passivating film is formed together with the lithium intercalation reaction at step (ii). The passivating film formed at this step contained a significant amount of organic film such as $EtOCO_2Li$, $(CH_2OCO_2Li)_2$, etc. Through the consecutive formation of passivating film at steps (i) and (ii), lithium intercalation into graphite proceeds smoothly without further decomposition of the organic electrolyte. © 1997 Published by Elsevier Science S.A.

Keywords: Ethylene carbonate; Diethyl carbonate; Graphite; Passivating films; Lithium compounds; Organic electrolytes

1. Introduction

The lithium-ion rechargeable battery has many intrinsic advantages such as high voltage and high energy density. The selection of organic electrolytes is one of the key issues in attaining high energy density and long cycle life as well as safety of battery. Concerning bulk properties of organic electrolytes for lithium batteries, we have reported approaches to design a suitable electrolyte system from the view point of solution chemistry [1,2]. Combinations of ethylene carbonate (EC) with lower viscosity solvents such as diethyl carbonate (DEC) and dimethyl carbonate (DMC) are commonly used for lithium-ion rechargeable batteries. In establishing the total performance of the lithium-ion battery, electrochemical stability and chemical stability including thermal stability of organic electrolytes are also very important parameters. This report focuses on the electrochemical stability of alkyl carbonate-based electrolytes and the characterization of the passivating layer formed on graphite.

The formation of a passivating film (SEI) on the surface of the carbon anode at the first charge is an important process in the lithium-ion system to allow lithium intercalation to proceed smoothly without further decomposition of the organic electrolyte. The surface chemistry of lithium intercalation in various carbon anodes has been studied by many researchers [3–8]. For example, Aurbach and co-workers [3,9,10] have studied the electrochemical intercalation of lithium into carbon anodes in various combinations of solvents, salts and additives on the basis of their research on surface chemistry between lithium metal and various electrolytes [11–14]. They concluded, using Fourier-transform infrared spectroscopy (FT-IR), that the passivating layers obtained in EC–DEC solutions containing $LiAsF_6$ and $LiClO_4$ were made of $(CH_2OCO_2Li)_2$ as a reduction product of EC and Li_2CO_3. The existence of $ROCO_2Li$ was also supported in the EC–DEC solution containing $LiPF_6$ as a salt. However, only qualitative analyses of the properties of the film have been reported in previous papers.

In this paper, quantitative analysis was examined for the characterization of passivating films formed on the graphite anode in EC–DEC solutions containing $LiClO_4$, $LiPF_6$ and $LiN(SO_2CF_3)_2$. The analytical methods used in this work are elemental analysis, temperature programmed decomposition

* Corresponding author.

PII S0378-7753(97)02619-0

mass spectroscopy (TPD–MS), Auger electron spectroscopy (AES), scanning electron microscopy (SEM), in situ X-ray diffraction (in situ XRD) and Fourier-transform infrared spectroscopy (FT-IR).

2. Experimental

In a lithium/graphite cell, the anode was lithium metal (Honjo Chemical) and the cathode was synthetic graphite (Timcal G&T, KS-44). The carbon electrode was prepared by coating the slurry of graphite powder and binder on a copper sheet by the doctor blade method. Graphite electrodes were tested in a parallel plate cell or coin cell. EC, DEC and DMC were used as received (Mitsubishi Chemical, battery grade). $LiClO_4$ and $LiPF_6$ were purchased from Tomiyama (battery grade) and used as received. $LiN(SO_2CF_3)_2$ (lithium bis-trifluoromethanesulfonylimide, LiTSNI) was purchased from 3 M and dried in a vacuum oven. The water and HF levels in the mixed electrolytes were measured by a moisture meter (Mitsubishi Chemical) and the alkali titration method, respectively. Typically, the water content in 1 M $LiClO_4$ or 1 M $LiN(SO_2CF_3)_2$/EC–DEC (1:1 by volume) was less than 10 ppm. 1 M $LiPF_6$/EC–DEC (1:1) solution contained less than 10 ppm of water and less than 40 ppm of HF.

Lithium intercalation was performed in a two-electrode cell with a lithium foil as both the counter and the reference electrodes. After the first discharge/charge operation, the carbon electrode was washed using dried DMC solvent in an argon glove box and placed into the SEM and AES chamber by using a transfer vessel after drying the sample. For the FT-IR measurement, very small pieces of the passivating film component were carefully collected by scratching the washed and dried graphite surface. The pellet was prepared by mixing the collected sample with high quality KBr in an argon glove box. The measurement was done under a H_2O- and CO_2-free atmosphere. The washed carbon electrode was soaked in water to completely dissolve the formed film on the graphite. This aqueous solution was used for the analysis of total lithium, fluorine and CO_2 (defined as inorganic carbon) content in the graphite after the first cycle. The content of total carbon (C_{total}) in the film was analysed as CO_2 by the complete oxidation of this aqueous solution. TPD–MS was carried out using the washed graphite electrode to analyse the composition of H_2O, CO_2 and hydrocarbon products in the film.

3. Results and discussions

Fig. 1 shows the relationship between the potential change and the XRD pattern of the graphite electrode during the first discharge by a real time in situ XRD method [15]. No lithium intercalation was observed until 0.55 V although reduction current was observed at the threshold potential of about 1.4 V versus Li/Li^+. The formation of the dilute stage 1 appeared

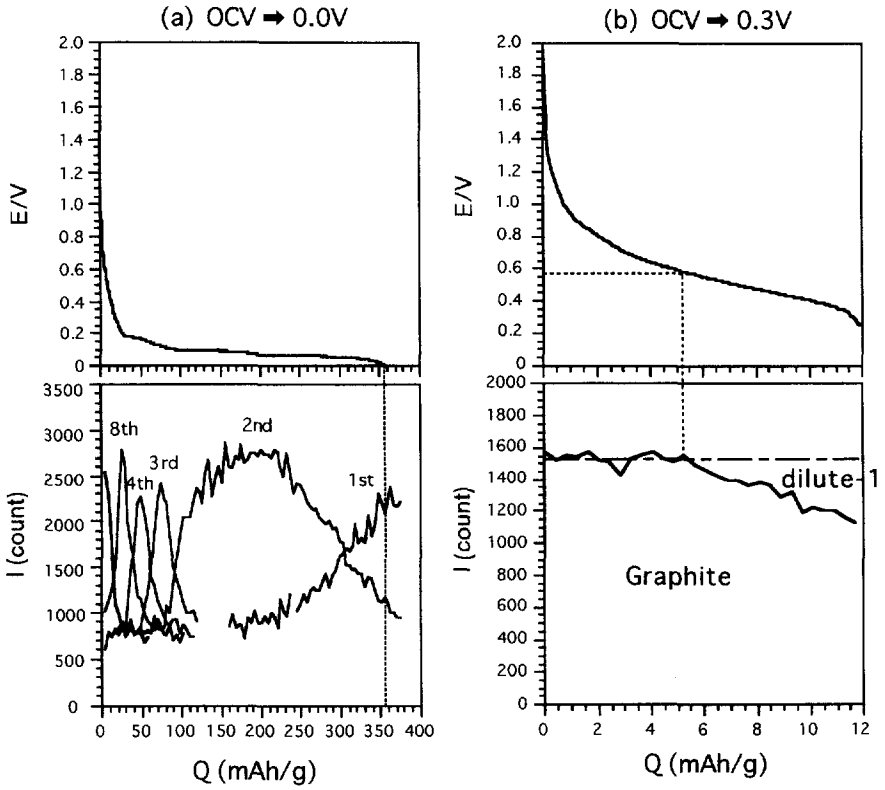

Fig. 1. Relationship between the potential and the XRD pattern change of graphite during the first discharge in the 1 M $LiClO_4$/EC-DEC system. The numbers in this figure indicate the various intercalation stage of graphite.

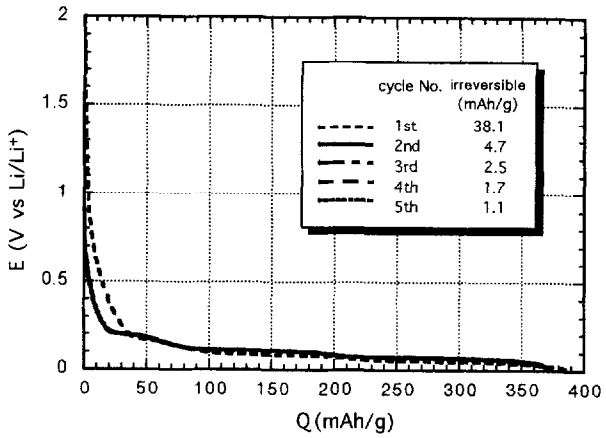

Fig. 2. Discharge curve during cycles in a coin-cell: electrolyte: 1 M $LiClO_4$/EC–DEC (2:8), discharge to 0.0 V at 0.2 mA/cm^2, charge to 1.5 V at 0.4 mA/cm^2.

at 0.55 V and the higher stages of lithium intercalation were observed from 0.55 to ~0.2 V. During the charge/discharge cycle in $LiClO_4$/EC–DEC, the potential curves after the second cycle were similar as shown in Fig. 2. Most of the irreversible capacity can be considered to be generated during the first cycle.

A reasonable explanation for these observations could be as follows: (i) the film formation reaction mainly occurs at the first discharge step, and (ii) the discharging process can be divided to the following three steps from the consideration of potential curve patterns and in situ XRD patterns: 'initial film formation step' (1.4 to 0.55 V); 'main film formation step' (0.55 to 0.2 V), and 'lithium intercalation step (0.2 to 0.0 V). The competitive reactions between film formation and lithium intercalation may occur at the main film formation step.

In order to characterize the passivating film formed during the three steps mentioned above, more quantitative analyses were examined as well as qualitative analyses by FT-IR, TPD–MS and AES. Fig. 3 presents the typical discharge/charge voltage profiles in the EC–DEC (1:1 by volume) electrolyte system containing 1.0 M of $LiClO_4$, $LiPF_6$ and

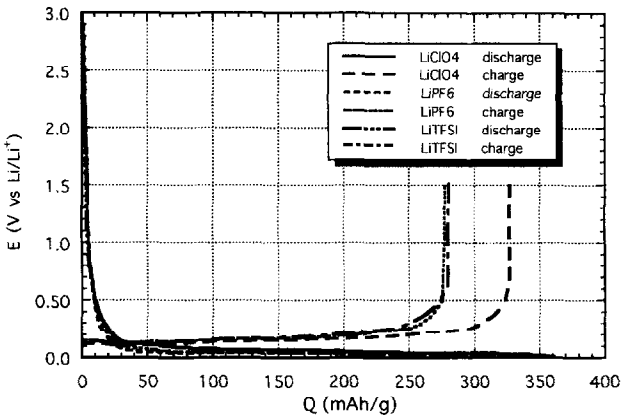

Fig. 3. First discharge/charge curves in various electrolytes: electrolyte: 1 M Li-salt/EC–DEC (1:1) discharge, to 0.0 V at 0.2 mA/cm^2, charge to 1.5 V at 0.4 mA/cm^2.

Table 1
Capacities in the first cycle and chemical composition of film formed after the first cycle

Salt	$LiPF_6$	$LiClO_4$	LiTFSI
Capacity (mAh/g)			
Discharge	303	358	314
Charge	268	320	272
Irreversible	35	38	42
Content in the film			
Li (μmol)	246	262	279
F (μmol)	34		3
Carbon analysis in the film			
C_{total} (μmol)	330	640	606
$C_{inorganic}$ (μmol)	85	221	190
$C_{organic}$ (μmol)	245	419	416
Molar ratio vs. Li			
F/Li (mol/mol)	0.14	0.0	0.0
C_{inorg}/Li (mol/mol)	0.35	0.84	0.68
C_{org}/Li (mol/mol)	1.00	1.60	1.49

LiTFSI. The effects of various lithium salts on discharge/charge capacities and irreversible capacity of graphite were observed as shown in Table 1. The orders of charge capacity in the first cycle were $LiClO_4 > LiPF_6 \simeq$ LiTFSI. Fig. 4 shows SEM photographs of the surface of the graphite electrode which was discharged to 0.0 V and then charged up to 1.5 V in the first cycle for these electrolyte systems. The graphite particles were covered with a passivating film not only at the edge plane but also at the basal plane of graphite. Typical morphologies of the films formed in the three electrolyte systems are rather similar (Fig. 4(a), (c) and (e)). However, it must be noted that the dissimilar morphologies were often observed at different sites on the same sample or in different examinations. The porous type of passivating layer was observed in the case of $LiClO_4$ and LiTFSI/EC–DEC systems (Fig. 4(d) and 4(f)). In the case of $LiPF_6$/EC–DEC, the film morphology consisted of globules of various sizes (Fig. 4(b)). The morphology in the different electrolytes resembles that resulting from lithium metal deposition [16].

Quantitative analysis was achieved by using the film samples obtained from the experiments as shown in Fig. 3. The lithium and fluorine contents in the films formed on the graphite electrodes after the first charge to 1.5 V are shown in Table 1. Results of carbon analysis of the aqueous solution into which the film component was dissolved are also shown in Table 1. The electron consumption used for irreversible capacities shown in Table 1 were almost equivalent to those used for the reduction of Li^+ found in the graphite for the three-electrolyte systems, respectively. These results strongly indicate that the electrons consumed during the discharge process are mostly used for one-electron reduction of Li^+ to form a passivating film. The ratio of inorganic carbon (C_{inorg}) and organic carbon (C_{org}) versus lithium atom are also shown in Table 1. C_{org} was calculated from the difference between C_{toal} and C_{inorg}. On the other hand, the lithium content in the electrodes was only 20–30 μmol in the samples which were

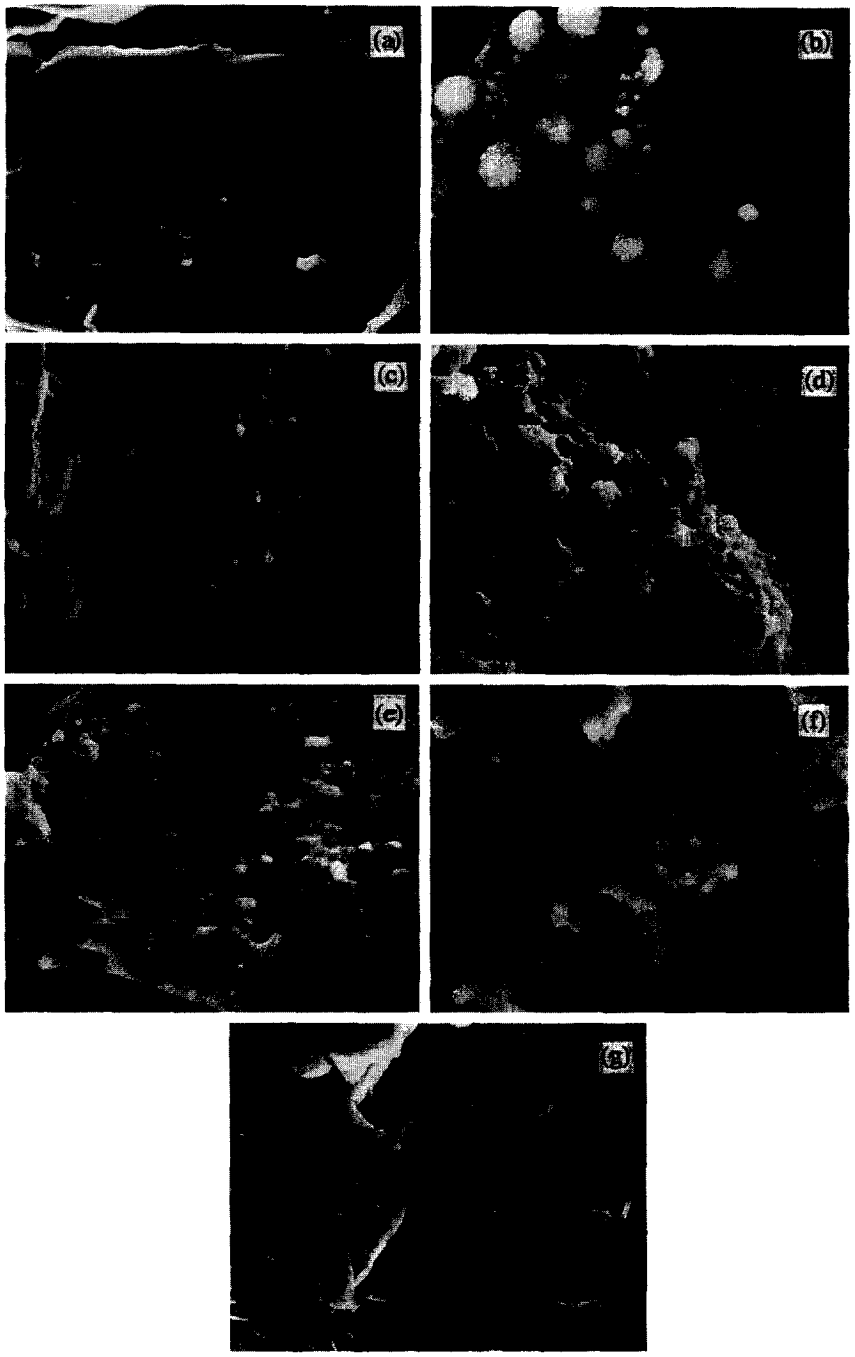

Fig. 4. SEM graphs obtained after the first cycle in (a, b) $LiPF_6$, (c, d) $LiClO_4$, (e, f) LiTFSI and (g) graphite before the first cycle; electrolyte: 1 M Li salt/EC–DEC (1:1), discharge to 0.0 V at 0.2 mA/cm^2, charge to 1.5 V at 0.4 mA/cm^2, (a), (c), (e), (g): ×10000, and (b), (d), (f): ×30000.

discharged to 0.55 V then charged to 1.5 V in the electrolyte systems. These results indicate that a significant amount of alkyl carbonate reduction products exist in the passivating films which were formed at the 'main film forming step' mentioned above. A fairly large amount of LiF was found in the case of the $LiPF_6$ system and a small amount of LiF in the LiTFSI system.

In order to characterize the film composition in more detail, TPD–MS of the graphite anodes after the first charge was carried out. Graphite electrodes after the first cycle were gradually heated to 200 °C. Decomposed products were collected in a cold trap and were analyzed by GC–MS. Gas chromatographs were shown in Fig. 5. EC and DEC are the components of electrolyte left in the film. DMC is the solvent for washing electrode. Significant amounts of H_2O, CO_2, ethanol, ethylene oxide and their derivatives such as dioxane and acetaldehyde were found in the decomposed products. The patterns of decomposed products were fairly similar in the different electrolyte systems. In addition, from the TPD–MS observation decomposition products such as ethanol, ethylene oxide and its derivatives were observed to be mainly produced in the temperature range from 50 to 200 °C. On the

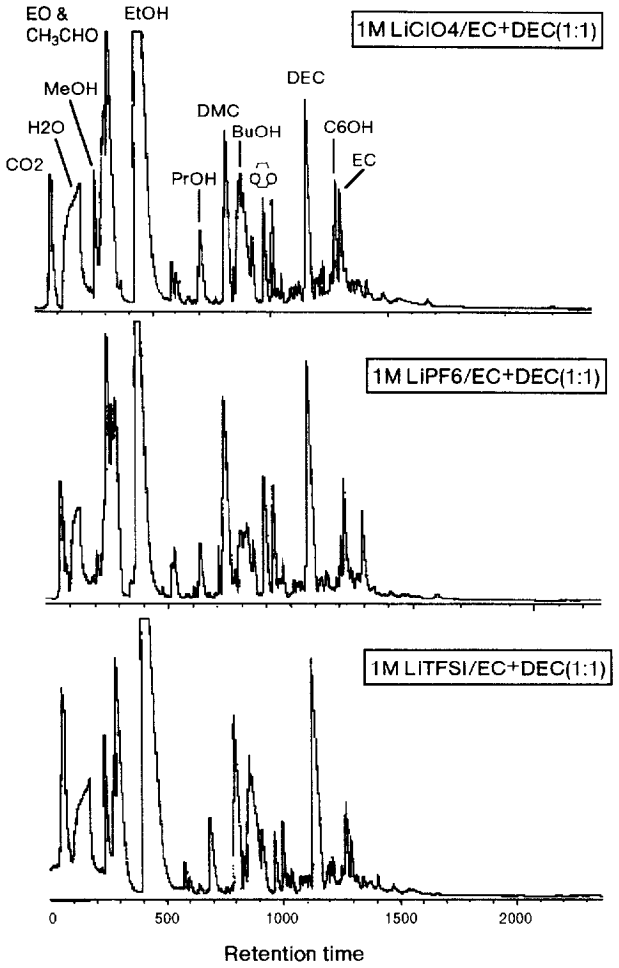

Fig. 5. Gas chromatograms of thermally decomposed products from graphite electrodes after the first charge.

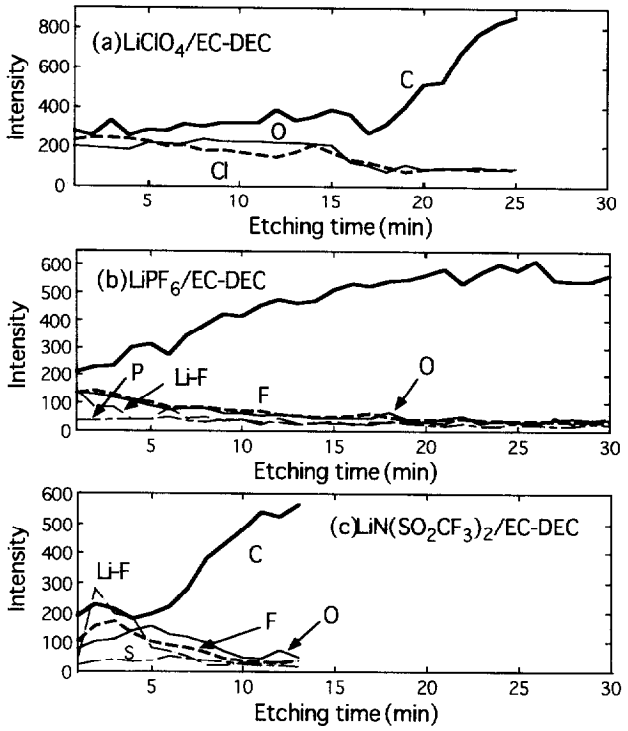

Fig. 7. Depth profiles of passivating film after the first charge in various electrolyte systems.

other hand, almost none of those organic products were found from the decomposed products in the graphite electrodes which were discharged to 0.55 V then charged to 1.5 V in the electrolyte systems, with the exception of H_2O and CO_2. During the first discharge in $LiClO_4$/EC–DEC system, ethylene, CO_2 and ethanol were detected by GC–MS.

These observations may confirm the formation of $ROCO_2Li$, $(CH_2OCO_2Li)_2$ and probably ROLi (R = Et or Me) in the main film formation step (from 0.55 to 0.2 V) mentioned above. The existence of these products was also supported by the FT-IR observations of film components as shown in Fig. 6. The IR bands from 600 to 1700 cm^{-1} indicate the existence of $ROCO_2Li$, $(CH_2OCO_2Li)_2$ and probably ROLi. The IR band around 2900 cm^{-1} corresponds to –CH stretching of the alkyl group [10,17].

Based on these observations, we propose the following film-forming mechanism on the graphite surface at the 'main film formation step': (i) the one-electron reduction of the solvated lithium cation basically occurs on the surface of graphite to produce a solvated lithium cation radical intermediate, and (ii) the intermediate is unstable and forms $ROCO_2Li$, $(CH_2OCO_2Li)_2$ and ROLi (R = Et or Me) on the

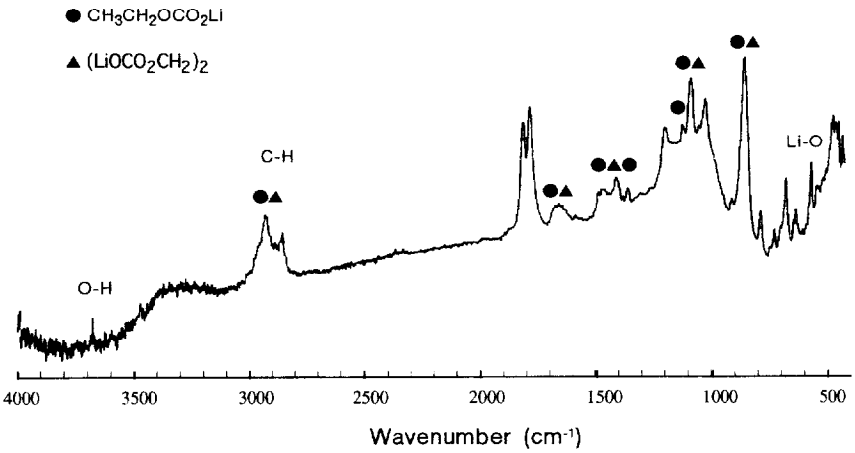

Fig. 6. FT-IR spectra of formed film after the first charge to 1.5 V in the 1 M $LiPF_6$/EC–DEC electrolyte.

graphite surface together with the decomposed gaseous products such as ethylene, CO_2, etc.

Depth profiles of elements in the films by AES are shown in Fig. 7. In the electrolyte systems, the carbon content near the surface of films was lower than inside the film layer. On the other hand, the fluorine content near the surface was relatively higher than inside in the case of $LiPF_6$ and LiTFSI systems. Chlorine was observed in the case of the $LiClO_4$ system. $ROCO_2Li$, $(CH_2OCO_2Li)_2$ and probably ROLi formed at 'film formation step' may partially react with HF included in the $LiPF_6$ electrolyte solution to form LiF. In the LiTFSI system, LiF was found in the film. This LiF is possibly formed by the reduction process of salt [18]. Phosphorus and sulfur were observed in the $LiPF_6$ and LiTFSI systems, respectively. However, it is difficult to recognize whether the decomposition products or the salt itself are left in the film since the quantity produced is so small. Lower discharge capacities of the $LiPF_6$ system as shown in Table 1 are probably due to the formation of LiF which has a high resistance for Li^+ migration.

4. Conclusions

The formation of a passivating film on the surface of graphite at the first charge is a very important process in the lithium-ion rechargeable battery to allow lithium intercalation to occur smoothly with stable charge and discharge cycles. The EC–DEC solvent system is one of the best electrolyte systems for this purpose. The electrochemical reactions in the first discharge process may occur through the following three different steps: (i) 'initial film formation step' from 1.4 to 0.55 V, (ii) 'main film formation step' from 0.55 to 0.2 V, and (iii) 'lithium intercalation step' from 0.2 to 0.0 V. In step (i), a small amount of electrolyte is reduced to form inorganic film-like Li_2CO_3. Most of the passivating film is formed together with the lithium intercalation reaction in step (ii). The passivating film formed in this step contains a significant amount of organic film such as $EtOCO_2Li$, $(CH_2OCO_2Li)_2$, etc. Through the consecutive formation of passivating film at steps (i) and (ii), the lithium intercalation reaction into graphite is able to proceed smoothly without further decomposition of the organic electrolyte.

References

[1] M. Ue and S. Mori, *J. Electrochem. Soc., 142* (1995) 2577.
[2] M. Ue and S. Mori, *Kinouzairyo, 15* (1995) 48; 50.
[3] D. Aurbach, Y. Ein-Eli, O. Chusid(Youngman), Y. Carmeli, M. Babai and H. Yamin, *J. Electrochem. Soc., 141* (1994) 603.
[4] J.O. Besenhard, M. Winter, J. Yang and W. Biberacher, *J. Power Sources, 54* (1995) 228.
[5] Z.X. Shu, R.S. McMillan and J.J. Murray, *J. Electrochem. Soc., 140* (1993) 922.
[6] R. Fong, U. von Sacken and J.R. Dahn, *J. Electrochem. Soc., 137* (1990) 2009.
[7] H. Yoshida, T. Fukunaga, T. Hazama, M. Terasaki, M. Mizutani and M. Yamachi, *Ext. Abstr., 36th Battery Symp. in Japan, 1995*, p. 101.
[8] M. Inaba, Z. Siroma, Z. Ogumi, T. Abe, Y. Mizutani and M. Asano, *Chem. Lett.*, (1995) 661.
[9] O. Chusid, Y. Ein-Eli, M. Babai, Y. Carmeli and D. Aurbach, *J. Power Sources, 43–44* (1993) 47.
[10] D. Aurbach, Y. Ein-Eli, B. Markovsky and A. Zaban, *J. Electrochem. Soc., 142* (1995) 2882.
[11] Y. Gofer, M. Ben-Zion and D. Aurbach, *J. Power Sources, 39* (1992) 163.
[12] D. Aurbach, A. Zaban, Y. Gofer, Y. Ein-Eli, I. Weissman, O. Chusid and O. Abramson, *J. Power Sources, 54* (1995) 76.
[13] D. Aurbach, Y. Ein-Eli and A. Zaban, *J. Electrochem. Soc., 141* (1994) L1.
[14] D. Aurbach, A. Zaban, A. Alexander, Y. Ein-Eli, E. Zinigrad and B. Markovsky, *J. Electrochem. Soc., 142* (1995) 2873.
[15] H. Asahina, M. Kurotaki, A. Yonei, S. Yamaguchi and S. Mori, *J. Power Sources*, submitted for publication.
[16] K. Kominato, E. Yasukawa, N. Sato, T. Ijuuin, H. Asahina and S. Mori, *J. Power Sources*, submitted for publication.
[17] D. Aurbach, M.L. Daroux, P. Faguy and E.B. Yeager, *J. Electrochem. Soc., 134* (1987) 1611.
[18] D. Aurbach, O. Chusid, I. Weissman and P. Dan, *Electrochim. Acta, 41* (1996) 747.